Design and experiment of a double-row self-propelled wheat plot planter

Yamei Feng[1,2,3], Shidong Deng[1,2,3], Xiupei Cheng[1,2,3*], Shuntao Sui[4*], Xiangcai Zhang[1,2,3], Zhongcai Wei[1,2,3], Xianliang Wang[1,2,3]

(1. *College of Agricultural Engineering and Food Science, Shandong University of Technology, Zibo 255000, Shandong, China*;
2. *Shandong Key Laboratory of Intelligent Agricultural Technologies and Smart Agricultural Machinery Equipment for Field Crops, Zibo 255049, Shandong, China*;
3. *Institute of Modern Agricultural Equipment, Shandong University of Technology, Zibo 255049, Shandong, China*;
4. *Key Laboratory of Agricultural Equipment Technology for Hilly and Mountainious Areas, Ministry of Agriculture and Rural Affairs, Chengdu 610000, China*)

Abstract: To address the challenges associated with the complex structure, poor sowing uniformity, and limited automation in plot breeding machinery, a double-row self-propelled wheat plot planter was designed, and an electronic control system was developed to manage plot seeding operations. This machine comprises the double-cone combined compartment tray-type seed-metering device, ditching and compacting device, self-propelled chassis device and electronic control system, which can complete the operation of ditching, seeding, and suppressing at one time. The electronic control system is centered around the STM32. The main method is to measure and control the operating speed of the seeder, then calculate the actual forward distance of the machine, and achieve automatic seed dropping in plots, fixed-length seeding, and control of the seed metering rotation speed. The optimization of the PID speed closed-loop feedback control algorithm, which precisely matches the rotational speed of the seed metering device with the operating speed of implement across different plot lengths, ensures accurate fixed-length seeding. The results of the soil trough test indicate that at an operating speed of 5 km/h and with the theoretical sowing length set to 2-8 m, the average control accuracy of actual plot sowing length exceeds 94%, and the variability coefficient of seeding depth is less than 10%. When the operating speed of seeder is 3-5 km/h, the coefficient of variation for seeding uniformity ranges from 26.18%-36.71%, remaining below 45%, thereby meeting the agronomic requirements for wheat plot seeding. The results of this study can serve as a reference for the design and optimization of wheat plot breeding trial equipment.

Keywords: wheat plot planter, self-propelled, seeding control, plot experiment
DOI: 10.25165/j.ijabe.20261901.9753

Citation: Feng Y M, Deng S D, Cheng X P, Sui S T, Zhang X C, Wei Z C, et al. Design and experiment of a double-row self-propelled wheat plot planter. Int J Agric & Biol Eng, 2026; 19(1): 132–142.

1 Introduction

Wheat, as a major global food crop, depends on the selection and breeding of superior varieties to enhance its yield[1,2]. Field breeding trials are crucial for screening and selecting wheat varieties with high productivity and broad adaptability, with plot sowing serving as a core component[3-5]. For a long time, plot seeding in field breeding trials has primarily relied on manual labor, which has problems such as high labor intensity, low operational efficiency, and challenges in ensuring seeding quality. In contrast, mechanical breeding offers advantages such as higher operational efficiency and more scientifically accurate breeding trial results. Consequently, investigating wheat plot seeding machinery holds great significance for enhancing the quality of breeding experiments[6,7].

Extensive research on plot seeding machinery has been undertaken by scholars both domestically and internationally, focusing on technological improvements and optimizations across various aspects[8,9]. In China, Yang et al.[10] developed a cone canvas belt-type seed-metering device and refined its key parameters. With the optimal parameter combination, the cone canvas belt-type seed-metering device effectively reduces seed damage and retention, offering certain insights for improving seed-metering device components in plot planters. Gong et al.[11] developed an electronic control system for plot planters to reduce the issue of inaccurate seeding lengths caused by ground wheel slippage, enhance the operational precision of the planter, and ensure the accuracy and reliability of breeding tests. Zha et al.[12] designed a novel air-suction seed metering device to address the problems of poor seed fluidity and low single-seed rate in conventional air-suction rice planters for small plots. This seed-metering device combines profiled suction holes with groove-based seed-disturbing elements, and the key parameters were optimized through discrete element simulation. In

Received date: 2025-02-27 **Accepted date:** 2025-12-28
Biographies: Yamei Feng, MS, research interest: modern agricultural equipment and computerized measurement and control, Email: 22503030074@stumail.sdut.edu.cn; **Shidong Deng**, MR, research interest: modern agricultural equipment and computerized measurement and control, Email: deng4do@163.com; **Xiangcai Zhang**, Associate Professor, research interest: intelligent agricultural equipment development, Email: zxcai0216@163.com; **Zhongcai Wei**, Associate Professor, research interest: modern agricultural equipment and computerized measurement and control, Email: weizc@sdut.edu.cn; **Xianliang Wang**, Associate Professor, research interest: modern agricultural equipment and computerized measurement and control, Email: wangxianliang2008@126.com.
***Corresponding author: Xiupei Cheng**, PhD, research interest: modern agricultural equipment and computerized measurement and control. College of Agricultural Engineering and Food Science, Shandong University of Technology, Zibo 255000, China. Tel: +86-13156988581, Email: cheng2021@sdut.edu.cn; **Shuntao Sui**, Senior Engineer, research interest: modern agricultural equipment. Key Laboratory of Agricultural Equipment Technology for Hilly and Mountainious Areas, MARA, Chengdu 610000, China. Email: 155046340@qq.com.

Austria, the Monoseed TC self-propelled single-seed plot planter and the Plotseed TC self-propelled plot planter, manufactured by Wintersteiger company, are among the most representative examples[13]. However, both plot planters are relatively large, requiring one operator to drive and another to assist with seed placement during operation, thereby reducing operational efficiency to some extent. Tabal et al.[14] developed a mechatronic single-row hand-pushed maize plot planter that utilized an electromechanical seed-casting device to achieve the seeding function. Comparative tests with three other breeding machines demonstrated that this seeding method excelled in both efficiency and cost-effectiveness. In summary, scholars both domestically and internationally have primarily focused on optimizing and improving the key components of existing plot planters, leading to some improvement in seeding performance. However, the current plot seeding machines still have the problems of large structure and difficulty in adapting to short-length plot seeding operations[15]. Meanwhile, the plot seed-metering device is driven by traditional mechanical mechanisms, the research on fully automatic seeding systems is limited, manual assistance is still required in the seed dropping process, and the accuracy of seeding operations is relatively low.

In view of this, considering the agronomic requirements for plot wheat sowing, this study designed a double-row self-propelled wheat plot planter in response to the existing plot planter with many manual assistance links, poor seeding uniformity, and insufficient automation level. The machine innovatively adopts a double-cone combined compartment tray-type seeding meter, which changes the seed sliding mode based on the traditional single cone to improve the dispersion uniformity of seeds. An electronic control system centered on the STM32 microcontroller was developed, with its hardware architecture and software modules designed to achieve automatic seed dropping, fixed-length seeding, and seed metering speed control. Through soil trough tests, the operation effects of the machine were explored under different operation speeds and different preset plot lengths to verify its feasibility. The research results of this paper can provide theoretical and technical support for the development and optimization of automated wheat plot seeders.

2 Materials and methods

2.1 Structure and working principle of the whole machine

2.1.1 Overall structure and working principle

The double-row self-propelled wheat plot planter consists of four main components: a double-cone combined compartment tray-type seed-metering device, a ditching and compacting device, a self-propelled chassis device, and an electronic control system, as shown in Figure 1a. The self-propelled chassis supplies the driving power for the machine, ensuring its stable operation. The double-cone combined compartment tray-type seed-metering device, positioned at the upper front of the whole machine, enables fixed-length seeding of quantitative seeds and serves as the core component of the planter. The ditching and compacting device, located under the double-cone combined compartment tray-type seed-metering device, performs ditching, soil covering, and suppressing, and the electric push rod is used to achieve lifting or lowering. Based on the operational requirements for plot seeding, a plot seeding electronic control system was designed to enable autonomous movement, automatic seed delivery, precise seed metering, fixed-length control, and furrow lifting control.

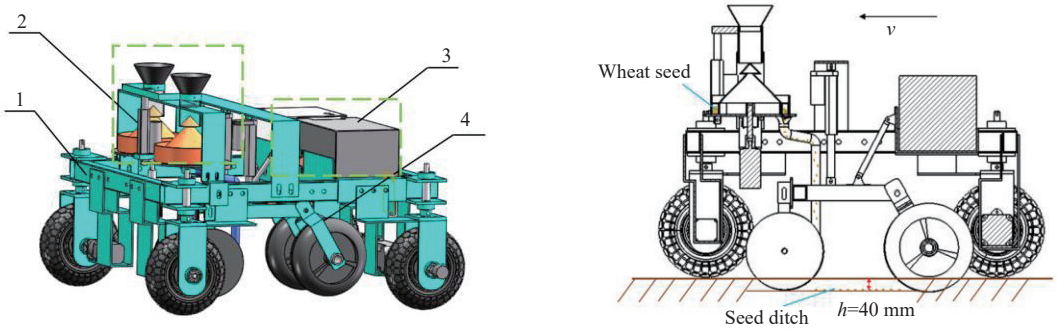

a. Overall structure b. Working principle

1. Self-propelled chassis device 2. Double-cone combined compartment tray-type seed-metering device 3. Electronic control system 4. Ditching and compacting device

Figure 1 Schematic diagram of overall structure and working principle of a double-row self-propelled wheat plot planter

The working principle diagram of the double-row self-propelled wheat plot planter is shown in Figure 1b, and v is the operating speed and h is seeding depth. According to the agronomic requirements of breeding test, a certain amount of wheat seeds were preset in the seed container. When working, the plot planter is activated, with the front and rear wheel stepper drive motors of self-propelled chassis rotating at the set speed to provide power for the whole machine. The electronic control system with a microcontroller at its core calculates the travel distance by using encoder speed measurement and machine's operating time, and determines the precise seed placement locations. Upon reaching the predetermined position, the seed-metering electric push rod is elevated, dispersing the wheat seeds from the seed container onto the compartment tray. At the same time, the double-cone combined compartment tray-type seed-metering device adapts to the machine's operating speed, and adjusts the rotational speed of seed metering to ensure complete seed discharge within the specified length. The ditching electric push rod lowers the ditching and compacting device to the appropriate position for trenching, and the wheat seeds are discharged from the seed discharge port, traveling through the seed discharge tube into the seed trench. The compacting wheel of the ditching and compacting device then covers the soil, ensuring that the seeds are firmly integrated with the soil, thereby completing the seeding operation. After seeding is completed in each plot, the space belt remains unsown, and the seeding operation for the next wheat variety begins when the machine reaches the preset position of the next plot.

2.1.2 Main technical parameters

The length of the breeding test plot typically ranges at 2-10 m. To enhance operability and portability, the design of the self-propelled wheat plot planter is compact, with shape dimensions of 1045 mm×1025 mm×785 mm. The key technical parameters are presented in Table 1.

Table 1 The key technical parameters of planter

Project	Value
Dimensions of form (Length×Width ×Height)/mm	1045×1025×785
Driving power/kW	3.46
Speed of operation/km·h^{-1}	3-6
Seeding row spacing/mm	200
Depth of seeding/mm	30-50
Number of rows	2

2.2 Key mechanism design

2.2.1 The double-cone combined compartment tray-type seed-metering device design

The key component of plot breeding machinery is the seed metering, whose seed distribution performance directly influences the seeding effectiveness of the field breeding test. Compared to large area field seeders, in addition to meeting the special requirements such as fixed-length sowing and interval sowing, plot planters require higher standards of seeding uniformity, compact structural design, and automation[16]. The conventional single-cone plot seed metering presents problems such as uneven seed distribution and a slow seed falling speed. To address these limitations, this study designed a double-cone combined compartment tray-type seed-metering device, as illustrated in Figure 2. It primarily consists of funnel, seed container lifting bracket, seed container, seed-metering device bracket, seed-metering motor bracket, electric push rod bracket, seed-metering motor, seed-metering coupling, propshaft, bottom plate, compartment tray-type, double-cone, and electric push rod. The seed container is in the form of a seed storage tube and can move up and down driven by an electric push rod.

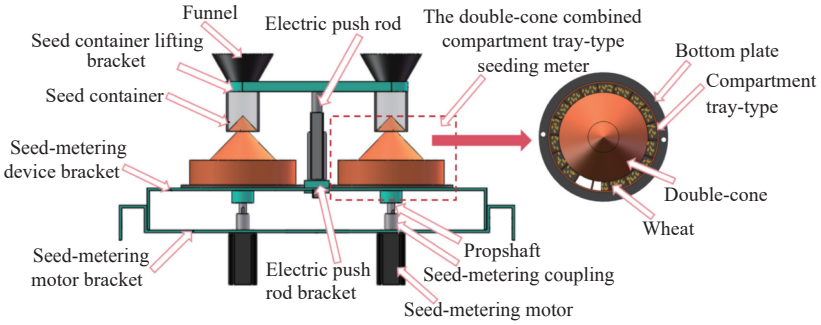

Figure 2 Diagram of the double-cone combined compartment tray-type seed-metering device

The double-cone is the core structure of the seed-metering device. This double-cone designed in the paper utilizes the height difference formed by the combination of upper cone and lower cone, which adds a throwing step to the seed sliding process. As a result, the seeds flowing out of the seed container can be quickly transformed from a piled state to a dispersed state, ultimately improving the uniformity of seed distribution on the compartment tray-type. The operation process of double-cone combined compartment tray-type seed-metering device seed dispenser can be divided into five links: lifting, falling, throwing, spreading, and metering, as shown in Figure 3. The lifting stage refers to the upward movement of the seed container, creating a gap between the double-cone. The falling stage refers to the process where the wheat seeds in the seed container slide down the upper cone due to the force of gravity. The throwing stage refers to the parabolic ejection of wheat seeds due to rotational force after they slide to the bottom of the upper cone. The spreading stage is the process of secondary dispersion, which occurs from the collision and impact between the ejected wheat seeds and the surface of the lower cone, thereby enhancing the uniformity of seed distribution and ensuring the consistency of seed number in the circular and uniformly distributed compartment trays. Finally, the metering stage involves the wheat seeds, which fall into the compartment tray-type and rotate with it, moving towards the seed-metering port, thus completing the seed metering operation.

Based on the preliminary research conducted for the device, the optimal parameters of the double-cone combined compartment tray-type seeding meter were determined to be the diameter of lower cone (D) is 173.23 mm,the inclination angle of lower cone (θ) is 45.78°, and the rotational speed of seed metering (n_1) is 4.43 r/min. In this case, the coefficient of variation for the uniformity of wheat seed dispersion was 8.75%, and the velocity of seeds entering the compartment tray-type was 1.03 m/s, meeting the mechanical requirements for wheat plot breeding[17].

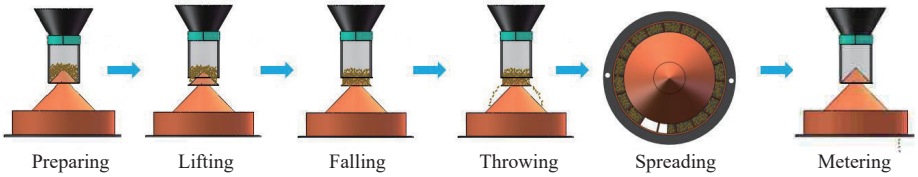

Figure 3 Operation process of double-cone combined compartment tray-type seed-metering device

2.2.2 The ditching and compacting device design

The ditching devices commonly utilized in wheat plot seeding machinery are typically categorized as double-disc, boot-type, or sliding knife ditching device[18,19]. During the ditching process, a larger angle of the disc ditcher results in a wider seed ditch. However, this also increases the operational resistance. If the disc angle is too small, an assembly issue may arise between the ditcher and the seed discharge tube, which could negatively affect the quality of ditching and the efficiency of soil backfilling. The ditching and compacting device developed in this study is depicted in Figure 4. It primarily consists of ditching electric push rod, seed-metering tube, double-disc ditching device, V-shaped compacting wheel, ditching and compacting connection frame, and pneumatic telescopic rod.

Based on the "Agricultural Machinery Design Manual" and classic design requirements[20], this research chose a double-disc

ditching device featuring a 210 mm diameter (D_1) and a 15° angle, which was combined with a V-shaped compaction wheel of 240 mm in diameter (D_2) to perform soil covering and compacting operations, ensuring a close bond between the soil and wheat seeds. The ditching electric push rod model was XTL100, with a maximum lifting force of 500 N and lifting speed of 24 mm/s. Precise control of lifting and lowering the ditching and compacting device is achieved through the telescopic action of electric push rods, while the lifting of ditching and compacting connection frame is assisted by a pneumatic telescopic rod.

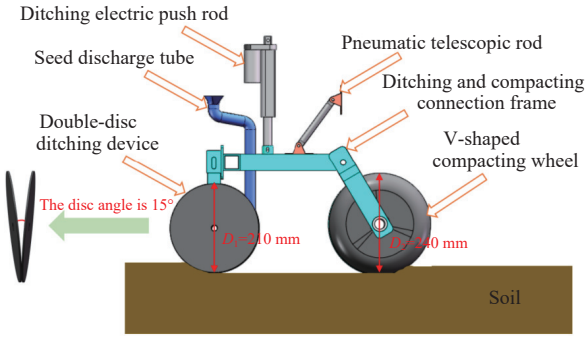

Figure 4 Diagram of the ditching and compacting device

2.2.3 The self-propelled chassis device design

Common driving modes of chassis include electric drive, hydraulic drive, and pneumatic drive[21]. Considering energy efficiency, environmental protection, and the feasibility of loading scheme, this study selects electric drive as the propulsion mode for the self-propelled chassis. The self-propelled chassis device, shown in Figure 5, primarily comprises frame, front drive wheel, front drive motor, front drive motor bracket, front wheel fixing plate, encoder, rear drive wheel, rear drive motor, rear wheel fixing plate, and rear drive motor bracket. To ensure the self-propelling capability of plot planter under pothole and uneven terrain conditions, a four-wheel drive mode is adopted. This effectively reduces the load on each drive wheel, thereby better achieving stable operation of the machine.

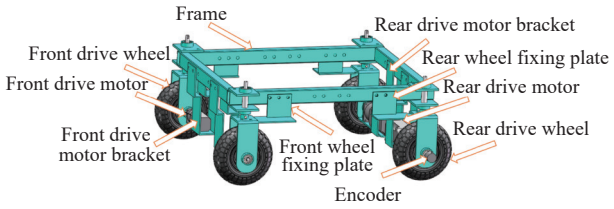

Figure 5 Diagram of self-propelled chassis device

During field operations, the drive motor delivers output torque to the drive wheels through a coupling, generating the driving force (F_q) needed to propel the implement forward. At the same time, the implement encounters opposing resistance from the soil. In accordance with the Law of the People's Republic of China on Soil and Water Conservation and the development of agricultural mechanization in hilly areas[22], crops should be cultivated on sloping land with a slope of less than 25°. Consequently, when the machine operates on a 25° slope, F_q required reaches its maximum.

At this point, F_q must be greater than or equal to the total resistance acting on the machine to ensure steady and uniform speed during the seeding operation, satisfying Equation (1). The coordinate system (OX_2Y_2) is established with the machine's center of gravity, and the force analysis of machine during constant-speed operation is illustrated in Figure 6.

$$F_q \geq F_K + F_a + F_\alpha + F_m + F_s \tag{1}$$

where, F_q is the driving force, N; F_K is the air resistance, N; F_a is the acceleration resistance, N; F_α is the slope resistance, N; F_m is the rolling resistance, which is related to the support force of slope (F_N) on the machine, N; F_s is the ditching resistance, N.

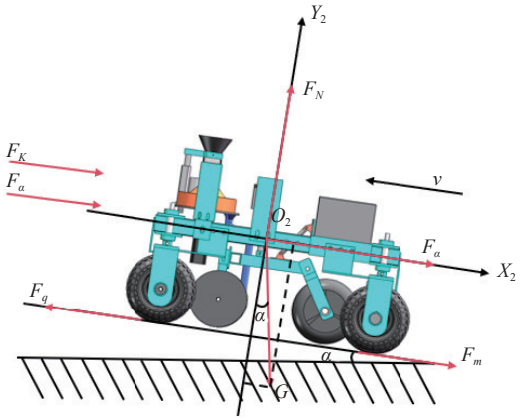

Figure 6 Diagram of the force analysis when operating steadily at a constant speed

The ground operating speed of wheat plot planter is 5 km/h. Due to its low speed and small windward area, the effect of air resistance can be disregarded. Given that the machine operates steadily at a constant speed, acceleration resistance can also be considered negligible. The calculation formulas for slope resistance and rolling resistance are presented in Equation (2):

$$\begin{cases} F_m = G \cdot f \cdot \cos\alpha \\ F_\alpha = G \cdot \sin\alpha \end{cases} \tag{2}$$

Where, G is the gravity of the machine, N; f is the rolling resistance coefficient; α is the travel acceleration, m/s^2.

Among them, the rolling resistance coefficient of wheeled agricultural machinery can be 0.05-0.1 when operating on dry land. In the actual operation of agricultural seeding, the ditching resistance generated by the soil's reaction on the ditching device must also be considered. The maximum ditching depth of the ditching and compacting device test is 50 mm. According to the reference[23], the average operating resistance is 13-20 N/cm. The total power consumed by the entire machine can be calculated using Equation (3):

$$P = \frac{(F_K + F_a + F_\alpha + F_m + F_s)v}{1000\eta} \tag{3}$$

where, v is the operating speed, m/s; η is the efficiency of power transmission through the coupling; P is the whole machine power, kw.

It is assumed that the walking speed of the machine is v= 5 km/h, and the transmission efficiency of the coupling is 99%. At this time, the total power consumed by the whole machine is 2.72 kw, which is less than the driving power of the machine 3.46 kw, and it can work normally. It should be noted that to ensure proper functionality of the machine on a 25° slope, the power supply must be upgraded to one that can provide higher power.

2.3 The electronic control system design

The control system comprises two components: hardware and software. The hardware primarily includes the control circuits of double-cone combined compartment tray-type seed-metering device, the self-propelled chassis drive circuit, and the ditching and compacting control circuit. The software includes the chassis driver

program, OLED interactive display program, encoder speed acquisition program, seed-metering speed control program, seed dropping control program, ditching and lifting control program, and PID(Proportional Integral Derivative) speed closed-loop feedback control algorithm.

2.3.1 Hardware design of electronic control system

In accordance with the operational requirements of the double-row self-propelled wheat plot planter, the hardware structural design of the control system is presented in Figure 7. It primarily consists of the chassis drive module, the seed dropping module, the seed discharging control module, and the ditching and lifting module. This research requires the output of 6 PWM(Pulse Width Modulation) pulse waveforms. Therefore, the STM32F103ZET6 microcontroller has been selected as the core to build the overall control system. The microcontroller features eight timers, which can efficiently drive each stepper motor and control the lifting operation of the electric push rod. The PID speed closed-loop feedback control algorithm is used to achieve precise control of the operating speed. Through coordination between the operating speed and the seeding speed, the seeding meter can accurately adjust the rotational speed. Simultaneously, key parameters such as plot length, plot interval length, machine operating distance, and speed are displayed in real time on the OLED interactive screen, enhancing the system's visualization and interactivity.

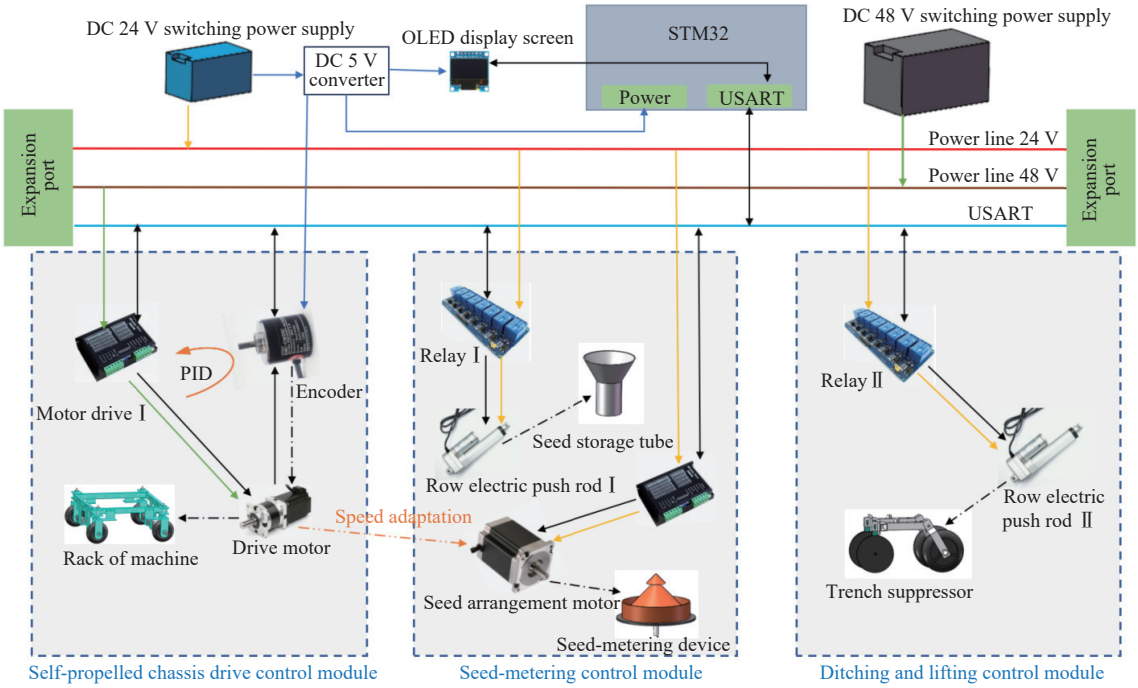

Figure 7 Hardware structure of the electronic control system

The front wheel drive motor is a direct current stepper motor of model 57HS, paired with a 10:1 reduction gearbox, and driven by a DM542 driver. The rear wheel drive motor is a direct current stepper motor of model 86BY, also coupled with a 5:1 reduction gearbox, and controlled by a DM860H driver. The E6B2-CWZ6C incremental encoder is connected to the rear drive wheel shaft via a coupling, used to measure the speed of the drive motor. The two seed motors are 3.1 N·m for stepper motors of model 57BY, with DM542 drivers selected for operation. Based on the requirement for minimal installation distance to avoid mechanical interference during operation, three 24 V electric push rods with a 100 mm stroke are selected for the lifting operations of the ditching and compacting device, as well as the double-cone combined compartment tray-type seed-metering device. The detailed parameters are listed in Table 2.

Table 2 Main parameters

Device	Model number	Nominal voltage/V	Nominal current/A	Output torque/N·m
Front wheel drive motor and gearbox	57HS100 Series	48	4.5	25
Rear wheel drive motor and gearbox	86BYG151 Series	48	6.5	54
Seed discharge motor	57BYG250 Series	24	4	3.1
Encoder	E6B2-CWZ6C	5	0.02	
Electric push rod	XTL100	24	2.1	

2.3.2 Software design of electronic control system

In this study, the Keil Vision 5 software was used to write the control system programs. These programs choose the C language selected as the programming language for the system. The flow chart of overall electronic control system is shown in Figure 8. The electronic control system needs to determine whether the predetermined sowing position has been reached in order to initiate the sowing operation. Next, the rotational speed of double-cone combined compartment tray-type seed-metering device is numerically related to both the operating distance and the preset seeding length of plots, ensuring that the seeding operation is completed within the specified length and improving the uniformity of seed metering.

According to the control process, once the control system is powered on and the system parameters are initialized, the user can use the buttons to set the parameters of the breeding plot length and the plot interval length. The set parameters, the operating distance, and the rear drive wheel speed acquired by the incremental encoder will be displayed one by one on the OLED screen. Automatic seed dropping is a prerequisite for the seeding operation of the machine after it enters the specified plot. In order to enable the system to complete the automatic fixed-point seed dropping operation, the design idea is to make a judgment based on the mathematical relationship between the actual operating distance of the machine, the length of seeding plot, and the interval length between plots.

The formula for determining whether the machine has reached the sowing starting position in the community is as follows:

$$\begin{cases} mod(L_q,(L_P+L_0)\le 0.05 \\ or \\ (L_P+L_0)-0.05\le mod(L_q,(L_P+L_0) \end{cases} \tag{4}$$

where, *mod* is the remainder function; L_q is the distance operated by the machine, m; L_P is the breeding plot length, m; L_0 is the plot interval length, m. In the formula, when the distance value distance between the machine and the preset sowing position of plot is within 0.05 m, the system determines that the machine has reached the automatic seed placement at fixed points. At this time, the electric push rod extends to drive the seed storage tube to rise, and the automatic seed dropping operation starts. After the seed dropping is completed, the electric push rod contracts to drive the seed storage tube back to its original position, waiting for the operation of the next plot.

According to the characteristics of plot sowing, there is a linkage matching relationship among the machine operating speed, the breeding plot length, and the speed of seed-metering device, and it is also related to the wheel diameter and the drive motor speed, as shown in Equation (5). This enables the derivation of the relationship model between the seed-metering motor speed and the drive motor speed, as shown in Equation (6).

$$\begin{cases} \dfrac{L_P}{v}=\dfrac{60}{n_1} \\ v=\pi dn \end{cases} \tag{5}$$

$$n_1=\frac{48.042n}{L_P} \tag{6}$$

where, n is the rotational speed of rear-wheel drive motor , r/min; d is wheel diameter of machine, d=255 mm; n_1 is the rotational speed of seed-metering device, r/min.

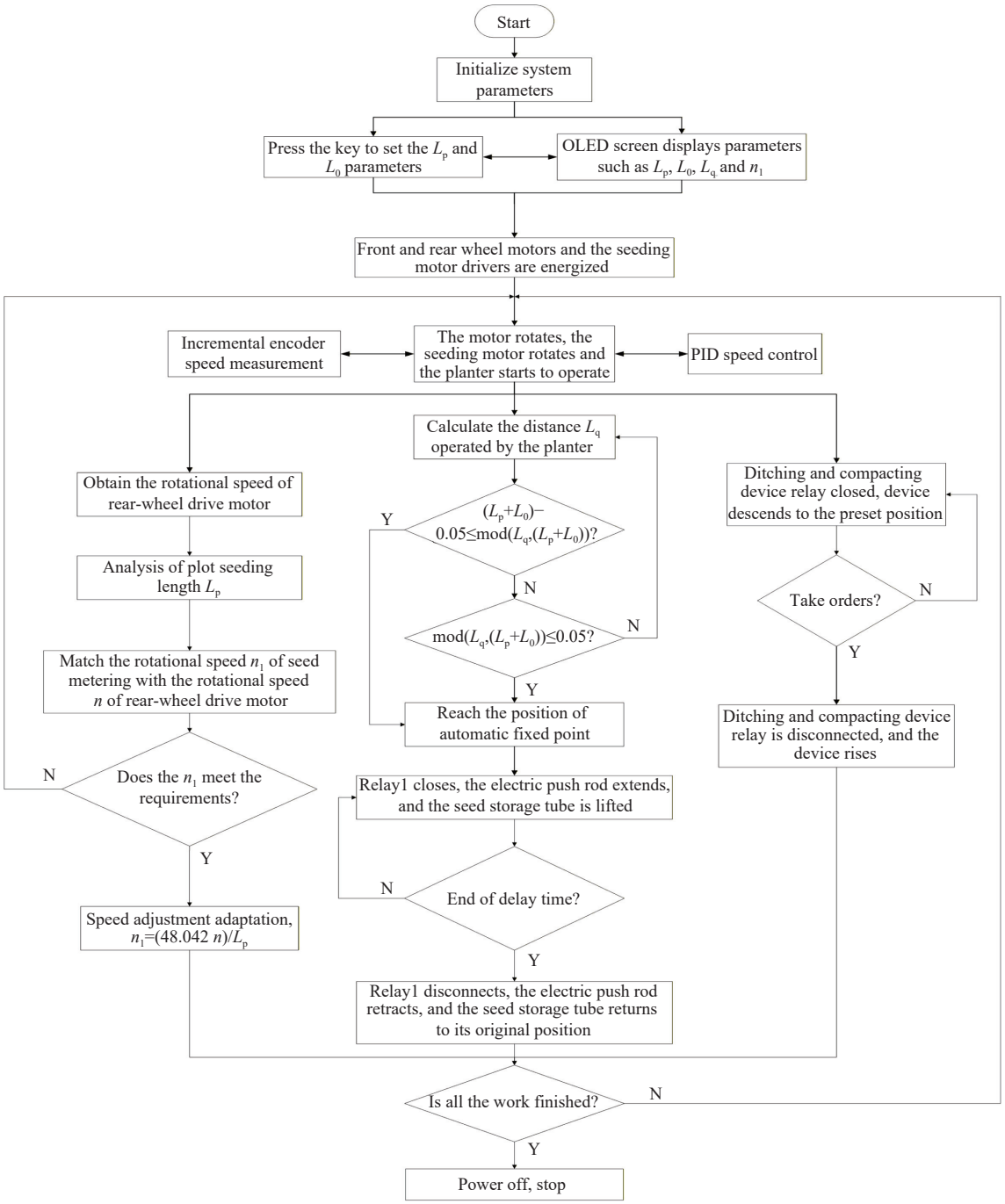

Figure 8 Overall electronic control system flow chart

2.3.3 PID speed closed-loop feedback algorithm

The control system employs a PID speed closed-loop feedback algorithm to regulate the speed of the rear drive motor, ensuring the linear motion of the machine and enabling precise matching control between the seeding meter speed and the machine operating speed, based on different plot lengths. In practical applications, the PID speed closed-loop feedback algorithm can quickly adjust the output signal through closed-loop feedback control of speed, enabling the system to respond rapidly to changes. Appropriate parameter values can effectively suppress system oscillations and errors, so that the machine can maintain stability. This method has been extensively utilized in the domain of machine control and motion[24-26]. The PID control principle diagram is shown in Figure 9.

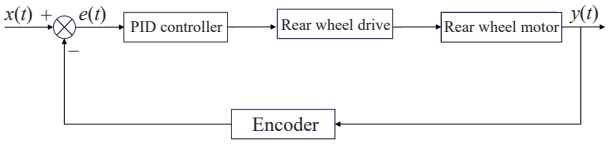

Note: $x(t)$ is the target speed of rear drive motor (r/min), $e(t)$ is the error(r/min), and $y(t)$ is the actual speed of rear drive motor (r/min).

Figure 9 PID control schematic diagram

In the closed-loop control of operating speed, the error $e(t)$ between the real-time operating speed $y(t)$, measured by the encoder at time t, and the set value $x(t)$ is input to the PID controller. The motor speed is then adjusted according to the PID control strategy to stabilize the speed near the set value. The rear wheel drive motor is a type 86 two-phase hybrid stepper motor, characterized by high nonlinearity, making it difficult to describe accurately[27]. Under ideal conditions, the transfer function model of motor is as follows:

$$G(s)=\frac{T^2L_di_A^2}{2Js^2+2bs+Z^2L_di_A^2} \tag{7}$$

where, T is the number of rotor teeth, T=50; L_d is motor inductors, H; i_A is A phase current, A; J is the moment of inertia, kg·cm^2; b is the brake damping coefficient, b=0.07.

It can be concluded that the response function of stepper motor is

$$G(s)=\frac{72.62}{s^2+0.0175s+72.62} \tag{8}$$

When the machine operates at speeds of 3 km/h, 4 km/h, and 5 km/h, the corresponding target rear-wheel drive speeds are 62 r/min, 83 r/min, and 104 r/min, respectively. By adjusting the parameters, the optimal settings for the PID controller were identified as K_p (Proportional coefficient) =12.72, K_i (Integral coefficient) =42.34, and K_d (Derivative coefficient) =0.93. At this point, the response times of the drive motor are 0.528 s, 0.566 s, and 0.631 s, with corresponding overshoot values of 11.18%, 11.17%, and 11.15%, respectively. It can be observed that as the operating speed of the machine increases, the response time of the drive motor also increases. However, the overshoot remains largely consistent, indicating that the control system demonstrates good stability. The PID response curve is illustrated in Figure 10.

2.4 Experimental environment and materials

To evaluate the operational performance of double-row self-propelled wheat plot planter, experimental research was conducted in the soil tank at the College of Agricultural Engineering Laboratory of Shandong University of Technology. The soil compaction within the 0-50 mm depth of the test soil tank was measured at 550 kPa, with a moisture content of 17.4%. The wheat variety used in the test was Jimai 22, and its thousand-grain weight was measured to be 47.23 g. The measuring ruler for seeding depth had an accuracy of 0.1 cm. The complete structure of the plot planter is depicted in Figure 11.

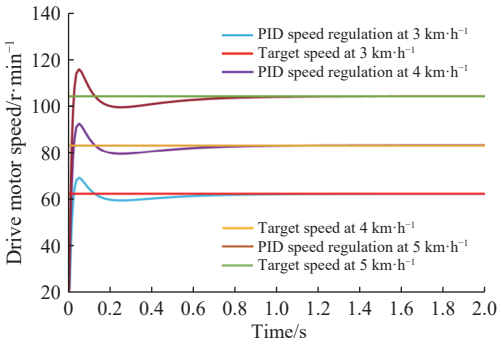

Figure 10 Diagram of PID response curve

Figure 11 Overall structure of plot planter

2.5 Experimental methods

To assess the operational performance of the plot planter, the operation length control accuracy test was carried out to evaluate the control effect of PID closed-loop speed feedback debugging algorithm. A seeding uniformity test was performed to assess the performance of double-cone combined compartment tray-type seeding meter and its synergistic effect with the adaptive operating speed adjustment method. Additionally, a seeding depth rate test was performed to assess whether the seeding depth could meet the requirements.

2.5.1 Operation length control accuracy test

In this paper, the encoder speed measurement method is used to obtain the operating speed of the plot planter. Combined with the preset plot sowing length, the rotational speed of the seed-metering device is then regulated in real time to meet the requirement that the seed-metering device rotates one turn within the specified length. Therefore, to analyze the control accuracy of operation length, the preset theoretical seeding length of plot was used as the test factor, and the actually measured sowing length of plot was used as the test index for verification. Based on the plot breeding operation length[28,29], the theoretical seeding lengths of plot were set to 2 m, 4 m, 6 m, and 8 m, with the machine operating speed fixed at 5 km/h. The actual distance operated was measured separately, each test was conducted five times, and the average values were subsequently recorded and calculated. During the test, the error between the actual and theoretical operation lengths was measured to evaluate the control effectiveness and accuracy of the machine fixed-length seeding. The test index was then calculated according to Equation (9).

$$A=\left(1-\frac{|L-L_P|}{L_P}\right)\times 100\% \tag{9}$$

where, A is the control precision, %; L is actually measured sowing

length of plot, m.

2.5.2 Seeding uniformity test

Taking the field wheat sowing rate of 135 kg/hm^2 as an example, when the theoretical operation lengths of the plot are 2 m, 4 m, 6 m, and 8 m, the number of seeds per row is 95, 190, 285, and 380, respectively. In the seeding uniformity test, the operating speed was used as the test factor, and the coefficient of variation for seeding uniformity served as the test index.

Based on the agricultural requirements for the wheat planter in the plot, the theoretical seeding lengths for the plot experiment were set to 2 m, 4 m, 6 m, and 8 m, with the walking speed of the machine set to 3 km/h, 4 km/h, and 5 km/h, respectively, to conduct the seeding uniformity experiment. Each group was repeated three times, and the average value was then calculated. Five measured segments were randomly selected from the plot, with each section measuring 200 mm in length, and the number of wheat grains was counted. The location of experimental sections was chosen to avoid areas with ground head, and the coefficient of variation for seeding uniformity was computed using Equation (10). The state of seeding uniformity measurement segment is shown in Figure 12.

Figure 12 Seeding uniformity measurement segment status chart

$$\begin{cases} B = \dfrac{S_D}{\bar{N}} \times 100\% \\ \bar{N} = \dfrac{\sum_{i=1}^{p} (x_i)}{p} \\ S_D = \sqrt{\dfrac{\sum_{i=1}^{p} (x_i - \bar{N})^2}{p-1}} \end{cases} \tag{10}$$

where, B is the coefficient of variation for seeding uniformity, %; S_D is the standard deviation of wheat seed count; $\bar{N}$ is the average number of wheat seeds in the measured segment, grain; p is the number of segments; x_i is the number of wheat seed grains in i^{th} measurement segment, grain.

2.5.3 Seeding depth test

In this experiment, the seeding depth at different plot lengths was measured, and the qualified rate of seeding depth was used as the experimental index for evaluation. Before starting the operation, the microcontroller sends instructions to the ditching relay, causing the relay to close. This activates the ditching push rod and the pneumatic telescopic rod, which descend along with the ditching and compacting device, setting the preset seeding depth to 40 mm.

The experiment was conducted twice in the soil tank, with theoretical operation lengths of 2 m, 4 m, 6 m, and 8 m, and a driving speed of 5 km/h. After each seeding operation, the seeding depth was measured relative to the surface after tillage, and 10 measuring points were randomly selected for the seeding depth experiment. The percentage of measured points with seeding depths within 40±5 mm relative to the total number of measured points was calculated, and the experimental index was determined according to Equation (11).

$$\begin{cases} C = \dfrac{C_1}{C_0} \times 100\% \\ \bar{C} = \dfrac{\sum_{j=1}^{q} (H_j)}{q} \\ S = \sqrt{\dfrac{\sum_{j=1}^{q} (H_j - \bar{C})^2}{q-1}} \\ V = \dfrac{S}{\bar{C}} \times 100\% \end{cases} \tag{11}$$

where, C is the qualified rate of seeding depth, %; C_1 is the qualified number of seeding depth; C_0 is the total number of measurement points; $\bar{C}$ is the average seeding depth, mm; q is the number of measured points; S is the standard deviation of the measurements; H_j is the seeding depth of measurement point j, mm; V is the stability coefficient of seeding depth.

3 Results and discussion

3.1 Operation length control accuracy test

In the control accuracy test for different plot sowing lengths, the PID speed closed-loop feedback control algorithm ensures that the drive motor starts smoothly, operates smoothly, and there is no jamming, achieving precise control of the actual sowing length in small plots. When the theoretical operation lengths are 2 m, 4 m, 6 m, and 8 m, the actual average operation lengths measured are 1.96 m, 3.98 m, 5.97 m, and 8.06 m, respectively. The average control accuracy of the system is 94.20%, 97.55%, 97.73%, and 96.65%, respectively, as shown in Figure 13.

The experimental results indicated that as the theoretical operation length increases from 2 to 6 m, the control accuracy of operation length gradually improves. However, due to the influence of machine inertia and the soil conditions, the improvement in control accuracy is limited. It is worth noting that when the theoretical operation length reaches 8 m, the control accuracy of the system decreases.

Specific analysis reveals that, under a theoretical operation length of 2 m, the short distance makes it difficult for the system to achieve accurate feedback regulation within the effective time. Additionally, the starting and stopping phases of the motor have a noticeable impact on the PID regulation, resulting in relatively low control accuracy. In the experiments with a theoretical operation length of 4-6 m, the PID control effect is significantly better than that under the 2 m condition. This is likely because the longer operating distance provides more time for the control system to adjust, allowing the feedback adjustment of the algorithm to be more fully utilized. The longer travel distance provides the system with sufficient feedback time to better compensate for errors during the initial stage, resulting in higher accuracy. However, the improvement in control accuracy is still limited. The experimental results for a theoretical operation length of 8 m show that as the travel distance increases, the system accumulates errors. Additionally, the longer operation time leads to an increase in the duration of machine vibration, which adversely affects the control performance, resulting in a decrease in control accuracy.

In the experiment with a theoretical operation length of 4 m, the comparison chart of actual operation length with and without PID speed closed-loop negative feedback control is shown in Figure 14. From the comparison, it can be seen that the actual average operation length without PID speed closed-loop negative feedback control is 3.692 m, with an error of 0.308 m and a control accuracy of 92.30%. The actual average operation length with PID speed closed-loop negative feedback control is 3.98 m, with an error of 0.02 m and a control accuracy of 97.55%. The control accuracy improves by 5.25%, indicating that the PID speed closed-loop feedback control significantly reduces the operation length error and enhances the system control accuracy. Compared with the traditional transmission method of gear and chain combination, the electronic control method can make the actual sowing length in the plot closer to the theoretical length and avoid significant fluctuations. This is consistent with the research results of Tang et al.[30] It should be noted that the actual sowing length in the plot is also closely related to the collision and bounce when the seeds fall. Therefore, appropriate measures should be taken in the future to avoid this.

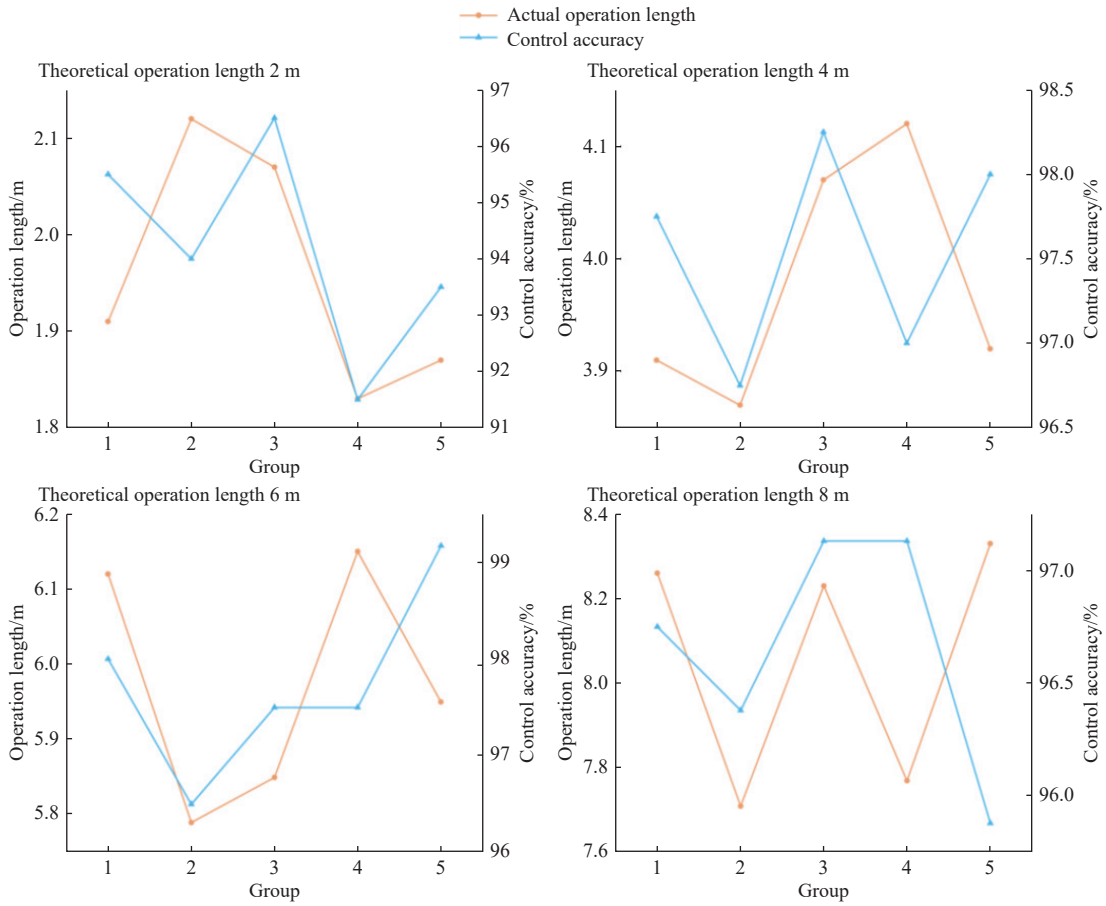

Figure 13 Operation length control accuracy test results chart

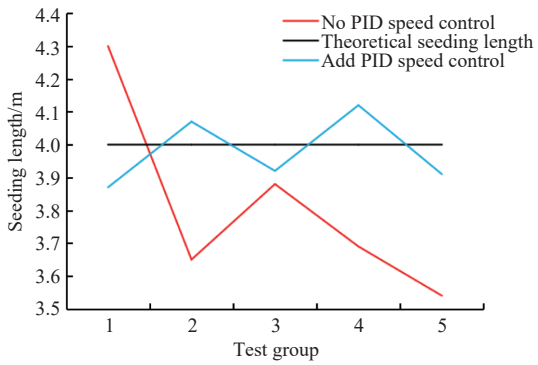

Figure 14 Comparison of test results between the control algorithm with and without PID speed closed-loop feedback

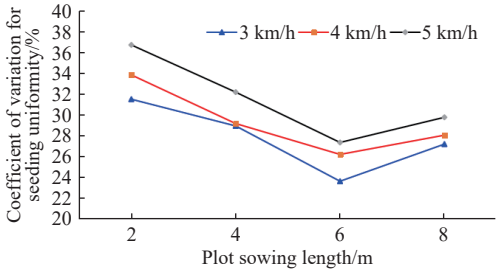

Figure 15 Test results of the coefficient of variation for seeding uniformity

3.2 Seeding uniformity test

In the seeding uniformity experiment, as the operating speed of the plot planter increases, the seeding motor speed also rises, subsequently influencing the seeding uniformity. The experiment results are shown in Figure 15.

When the theoretical operation length remains intact, an increase in the machine operation speed leads to a gradual rise in the variation coefficient of plot seeding uniformity, indicating that the seeding uniformity decreases as the operation speed increases. When the plot length was set to 6 m, the coefficient of variation in plot seeding uniformity increased from 23.60% to 27.33% as the operating speed rose from 3 to 5 km/h, a rise of 3.73 percentage points. At other lengths, a similar improvement is observed. This

may be due to the fact that, as the operating speed of the machine increases while the plot length remains unchanged, the seeding motor speed decreases, leading to reduced stability in continuous rotation and a diminished ability to overcome rotational resistance. Furthermore, as the traveling speed of the implement increases, its vibration also intensifies. This, coupled with the potential impact of ground unevenness, leads to a gradual rise in the coefficient of variation for seeding uniformity.

When the operating speed is constant, the variation coefficient of seeding uniformity for different theoretical operation lengths first decreases and then increases. For short theoretical operation lengths, the seed-metering operation speed is relatively fast, the disorder of seeds increases, and the ability of the PID control algorithm to adjust the speed of drive motor is limited, which results in a relatively large coefficient of variation in sowing uniformity. At plot seeding length of 2 m, the coefficient of variation for seeding uniformity exceeds 30%. However, for excessively long operation lengths, the seeding speed decreases, and system stability is reduced, leading to an increase in the coefficient of variation for seeding uniformity. According to the NY/T996-2006 Quality Standard for Wheat Fine Seed Planter Operation, the coefficient of variation for wheat seeding uniformity for large-field mechanized is 45%. For the research results of this paper, when the machine operating speed is 3-5 km/h, the coefficient of variation for seeding uniformity is 26.18%-36.71%, all lower than 45%, so it meets the performance specification requirements. Compared with the traditional plot seeding machine that uses a combination of chain drive and gear drive, the electronic control method can overcome the shortcomings of mechanical drive and effectively improve the seeding uniformity, which is consistent with the research results of Zhang et al.[31]

3.3 Seeding depth test

In the seeding depth test, the soil ditching and seeding conditions were observed, and there was no significant piling of seed grains in the ditch. The experimental measurements of seeding depth are presented in Figure 16, with the corresponding results shown in Figures 17 and 18.

Figure 16 Measurement of seeding depth

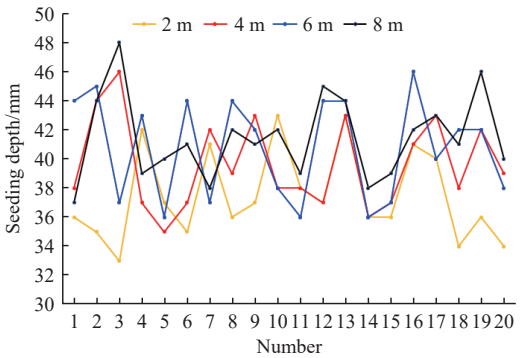

Figure 17 Seeding depth results at different measurement points

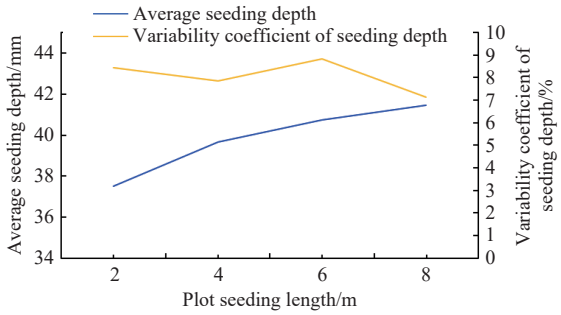

Figure 18 Results of average seeding depth and variability coefficient of seeding depth

The analysis of results indicates that the seeding depth is 33-46 mm, the average sowing depth is 37.5-41.7 mm, the sowing stability coefficient is 90.97%-93.40%, and the coefficient of variation is 6.60%-9.03% at different lengths. Furthermore, the qualified rate of seeding depth was more than 80%, which met the agronomics requirements of wheat plot seeding. Comprehensive experiments demonstrate that although the actual seeding depth is subject to fluctuations due to equipment vibration and terrain variations, the seeding depth qualification for all operation lengths exceeds 90%, except for the 2 m length.

4 Conclusions

(1) In this paper, a double-row self-propelled wheat plot planter was designed, which included the double-cone combined compartment tray-type seed-metering device, the self-propelled chassis device, the ditching and compacting device, and the electronic control system. The key components and parameters of the plot planter were designed and determined to meet the operating requirements.

(2) This paper develops an electronic control system for plot seeding. The system adopts the STM32F103ZET6 microcontroller as the core, the encoder as the speed measurement element, and the different types of drive motors and electric push rods as the execution elements, so as to realize the automatic control operation of each link of plot seeding. The PID speed closed-loop feedback control algorithm was implemented with tuning parameters set as K_p=12.72, K_i=42.34, and K_d=0.93. When the machine operating speed is 3-5 km/h, the corresponding response time of drive motor is 0.528-0.631 s, and the overshoot values are less than 11.18%, respectively. The result showed that the speed control accuracy is high, which lays a foundation for the precise control of plot seeding.

(3) The results of experiments indicate that with theoretical plot seeding lengths of 2 m, 4 m, 6 m, and 8 m, and an operating speed of 5 km/h, the control accuracy of actual plot sowing length is 94.20%-97.73%, the sowing depth is 33-46 mm, and the variability coefficient of seeding depth is 6.60%-9.03%. When the machine operating speed is 3 km/h, 4 km/h, and 5 km/h, the coefficient of variation for seeding uniformity is 26.18%-36.71% at the plot seeding length of 2-8 m, which meets the agronomic requirements for a wheat plot planter.

Acknowledgements

This work was supported financially by the Shandong Province Natural Science Foundation (Grant No. ZR2023QE040); the Key Laboratory of Agricultural Equipment Technology for Hilly and Mountainous Areas, Ministry of Agriculture and Rural Affairs, China (Grant No. 2022KLOP06); the Start-up Fund for Doctor of Science for Technology of Shandong University of Technology

(Grant No. 421029); the Innovation and Entrepreneurship Education Reform Project: Application of TRIZ innovation method in the research of mechanized seeder; the Shandong Province Natural Science Foundation (Grant No. ZR2025MS975); and the National Natural Science Foundation of China (Grant No. 32572226).

[References]

[1] Fei S P, Chen Z, Li L, Ma Y T, Xiao Y G. Bayesian model averaging to improve the yield prediction in wheat breeding trials. Agricultural and Forest Meteorology, 2023; 328: 109237.

[2] Abdallah A D, Liao Q X, Ibrahim E J, Wang L. Design and experiment of the pneumatic cylinder type precision metering system for wheat. Int J Agric & Biol Eng, 2023; 16(5): 88–94.

[3] Li L, Wang J Y, Li C N, Mao X G, Zhang X Q, Sun J W, et al. Insights into progress of wheat breeding in arid and infertile areas of China in the last 14 years. Field Crops Research, 2024; 306: 109220.

[4] Pérez-Ruiz M, Prior A, Martinez-Guanter J, Apolo-Apolo O E, Andrade-Sanchez P, Egea G. Development and evaluation of a self-propelled electric platform for high-throughput field phenotyping in wheat breeding trials. Computers and Electronics in Agriculture, 2020; 169: 105237.

[5] Li J Q, Huang Z S, Jiang Y C, Cui Z J, Zhang M Z, Zang Y, et al. Design and test of a precision air-suction maize seed-metering device for plot planting based on CFD-DEM coupling. Computers and Electronics in Agriculture, 2025; 238: 1–24.

[6] Gao Y, Wang D C, Fang X F, Zhao J Z, Wang G H, Wang Z. Optimal matching of transmission system for multi-purpose self-propelled pasture plot operation machine. Transactions of the CSAM, 2012; 43(S0): 11–18, 23. (in Chinese)

[7] Xing Q S, Ding S, Xue X Y, Cui L F, Le F X, Fu J. Design and testing of a clamping manipulator for removing abnormal plants in rape breeding. Applied Sciences, 2023; 13: 9723.

[8] Li Z D, Wu J J, Quan Z, Duan D L, Zhang T, Liu L C, et al. Research on the impact of wheat seed collisions on the distribution performance of an air-assisted centralized distribution device based on CFD-DEM numerical simulation. Computers and Electronics in Agriculture, 2024; 225: 109241.

[9] Yuan X Y, Huang C J, Tao G X, Yi S J, Li Y F. Design and experiment of oil-electric hybrid air-suction sorghum plot seeder. Agriculture, 2024; 14: 432.

[10] Yang R B, Zhang X, Li J D, Shang S Q, Chai H H. Parameter optimization and experiment on cone canvas belt type seed-metering device. Transactions of the CSAE, 2016; 32(3): 6–13. (in Chinese)

[11] Gong L N, Yuan Y L, Shang S Q, Jiang J L, Zheng Y N. Design and experiment on electronic control system for plot seeder. Transactions of the CSAE, 2011; 27(5): 122–6. (in Chinese)

[12] Zha X T, Li J Y, Zhao H J, Chen L, Yang W, Yang R B, et al. Design optimization of an air-suction type seeder for rice breeding plots based on the discrete element method (DEM). Smart Agricultural Technology, 2025; 12: 1–17.

[13] Shang S Q, Yang R B, Yin Y Y, Guo P Y, Sun Q. Current situation and development trend of mechanization of field experiments. Transactions of the CSAE, 2010; 26(Z1): 5–8. (in Chinese)

[14] Tabal R E, Amongo R M C, Quilloy E P, Peralta E K. Development of a single-row push type plot seeder with mechatronic seed feeding device for corn (*Zea mays* L.) field breeding experiment. IOP Conference Series: Earth and Environmental Science, 2022; 977: 012067.

[15] Lian Z G, Wang J G, Yang Z H, Shang S Q. Development of plot-sowing mechanization in China. Transactions of the CSAE, 2012; 28(Z2): 140–5. (in Chinese)

[16] Shang S Q, Wu X F, Yang R B, Li L Y, Yang X L, Chen D. Research status and prospect of plot-sowing equipment and technology. Transactions of the CSAM, 2021; 52(2): 1–20. (in Chinese)

[17] Feng Y M, Deng S D, Cheng X P, Sui S T. Design and parameter optimization of a double-cone wheat plot seed-metering device based on EDEM. Engenharia Agrícola, 2024; 44: e20240077.

[18] Ma X, Kuang J X, Qi L, Liang Z W, Tan Y X, Jiang L K. Design and experiment of precision seeder for rice paddy field seedling. Transactions of the CSAM, 2015; 46(7): 31–37. (in Chinese)

[19] Malasli M Z, Celik A. Disc angle and tilt angle effects on forces acting on a single-disc type no-till seeder opener. Soil and Tillage Research, 2019; 194: 104304.

[20] Zang Y, Luo F, Huang Z S, Jiang Y C, Li J Q, Zhang M H. Design and experiment of combined rice-wheat dual-purpose sowing furrow opener. Transactions of the CSAE, 2025; 41(19): 42–53. (in Chinese)

[21] Wang B Y, Zhu J X, Chai X L, Liu B, Zhang G W, Yao W. Research status and development trend of key technology of agricultural machinery chassis in hilly and mountainous areas. Computers and Electronics in Agriculture, 2024; 226: 109447.

[22] Hu Z C, Zhang M, Luo W W, Pang Y L, Lang F N, Li Q S. Advancing agricultural mechanization in China's hilly and mountainous areas: Key strategies and technological focus. Transactions of the CSAE, 2025; 41(14): 39–50.

[23] Botta G F, Tolon-Becerra A, Tourn M, Lastra-Bravo X, Rivero D. Agricultural traffic: Motion resistance and soil compaction in relation to tractor design and different soil conditions. Soil and Tillage Research, 2012; 120: 92–98.

[24] Wang H Y, Fan J Y, Wang L J, Wu J H, Wang W, Yang C C. Design and test of the temperature control system for the feed pelleting and conditioning based on PID. Transactions of the CSAE, 2023; 39(1): 1–8. (in Chinese)

[25] Yu C C, Li H W, He J, Chen G B, Lu C Y, Wang Q J. Design and experiment of high-frequency intermittent fertilizer supply system based on PID algorithm. Transactions of the CSAM, 2020; 51(11): 45–53, 63. (in Chinese)

[26] Zhang C L, Wu R, Chen L Q. Design and test of electronic control seeding system for maize. Transactions of the CSAM, 2017; 48(2): 51–59. (in Chinese)

[27] Fu H M, Huang X Y, Qiu G J, Chen D. Powder feeding accuracy control of screw feeding mechanism based on fuzzy PID. Packaging Engineering, 2023; 44(23): 164–170.

[28] Bagarello V, Ferro V. Analysis of soil loss data from plots of differing length for the Sparacia experimental area, Sicily, Italy. Biosystems Engineering, 2010; 105: 411–422.

[29] Bagarello V, Ferro V, Giordano G, Mannocchi F, Pampalone V, Todisco F, et al. Effect of plot size on measured soil loss for two Italian experimental sites. Biosystems Engineering, 2011; 108: 18–27.

[30] Wang H, Dong Z Z, Zhao J B, Tang Y W, Wang M L. Research on high precision plot seeding system based on stroke self calibration. Journal of Agricultural Mechanization Research, 2020; 3: 143–147. (in Chinese)

[31] Xue C, Chen L Q, Zhang C L, Liu C, Zhang L Y, Zhu J W. Design and experiment of wheat plot seeder control system based on Beidou fault-tolerant strategy. Transactions of the CSAM, 2025; 56(3): 240–246, 362. (in Chinese)